

# Development of a heat exchanger for cogeneration via TEG

Björn Pfeiffelmann<sup>1</sup>, Michael Diederich<sup>2</sup>, Ali Cemal Benim<sup>1\*</sup>, Andreas Hamberger<sup>2</sup> and Markus Heese<sup>2</sup>

<sup>1</sup>Center of Flow Simulation (CFS), Department of Mechanical and Process Engineering,  
Duesseldorf University of Applied Sciences, D-40476 Duesseldorf, Germany

<sup>2</sup>Endress Holzfeuerungsanlagen, D-91593 Burgbernheim, Germany

**Abstract.** To develop an innovative cogeneration biomass boiler, which uses thermoelectric generators (TEG), a simplified model of the heat exchanger is created and the design is optimized. The boiler with a thermal power of 200 kW will partly convert the heat into electricity. The maximum temperature of the hot side of the TEG should not exceed 300°C to avoid damage. While holding these requirements the cost and the installation space of the heat exchanger should be as low as possible, with a minimal effort for the flue gas blowers at once. Following these objectives, the simplified heat exchanger model is optimized with NOMAD optimization algorithm. Out of the resulting Pareto front two heat exchanger designs are discussed.

## Nomenclature

|                  |  |
|------------------|--|
| A                | Area [m <sup>2</sup> ]                             |
| D                | Hydraulic diameter [m]                             |
| f                | Friction coefficient                               |
| ff               | Filling factor                                     |
| h                | Channel height [m]                                 |
| k                | Thermal conductivity [W/mK]                        |
| L                | Channel length [m]                                 |
| m <sub>h</sub>   | Slope of h in flow direction                       |
| m <sub>ff</sub>  | Slope of ff in flow direction                      |
| n <sub>TEG</sub> | Total number of TEG                                |
| Nu               | Nusselt number                                     |
| Pr               | Prandtl number                                     |
| r                | Radius [m]   |
| t                | Spreader plate thickness [m]                       |
| Re               | Reynolds number                                    |
| R <sub>p</sub>   | Spreading resistance [K/W]                         |
| R <sub>s</sub>   | R <sub>p</sub> based on hot spot temperature [K/W] |
| R <sub>1D</sub>  | One dimensional thermal resistance [K/W]           |
| V                | Volume [m <sup>3</sup> ]                           |
| w                | Channel width [m]                                  |

## Greek Symbols

|   |                         |
|---|-------------------------|
| ε | aspect ratio            |
| τ | dimensionless thickness |

## Subscripts

|    |                       |
|----|-----------------------|
| c  | Center of heat source |
| g  | Gas                   |
| h  | Hot surface of TEG    |
| m  | mean                  |
| la | laminar               |
| p  | Spreader plate        |
| s  | Heat source/sink      |
| tr | transitional          |
| tu | turbulent             |

## Abbreviations

|     |                          |
|-----|--------------------------|
| ORC | Organic Rankine Cycle    |
| TEG | ThermoElectric Generator |

## 1 Modelling

Combustion is still a main process for the generation of power and heat [1-6]. With respect to solid fuels, the gasification technology is additionally applied [7]. Along with the endeavours for the utilization of renewable energies [8,9], as well as recovery techniques [10] combined with heat transfer augmentation technologies [11,12], combustion persists to play an important role in the area of renewable energies. This is due to the fact that the biomass, which is a renewable fuel, is also converted by combustion [13,14].

Indeed, using the combustion of biomass for heating buildings is environmentally friendly compared to common energy sources like oil and gas. This is due to the renewable characteristic of biomass, especially in the case of using waste wood e.g. from joinery [15].

Traditional biomass boiler are losing the major part of exergy when they are operating [16]. Chemical exergy is saved in the biomass and by converting it into heat via combustion and saving the heat into heating water the exergy content reduces strongly. Larger biomass power plants are creating steam [17] and electric power using a turbine. This reduces the exergy loss but cannot easily be downsized remaining economically feasible. For biomass power plants in the range of 100 kW to 1000 kW cogeneration is seldom [18]. There are various technologies, which have the potential to fill this gap but are not implemented in commercial products yet e.g. Organic Rankine Cycle (ORC) [19,20] or Stirling engine [21].

The present investigation focuses on the usage of thermoelectric generators (TEG) to recover the created heat into electricity [22]. By applying a temperature gradient onto a TEG, the heat flowing through it, is

partly converted into electricity. The conversion efficiency is, with 3-5%, relatively low, but this is equalised by the negligible maintenance effort and free scalability. The first mentioned is reasoned by the lack of moving parts and the latter by modularity of TEG modules.

Over the past decades, there has been a high amount of interest in combustion driven thermoelectric power systems. This has been reviewed by Mustafa et. al. [23]. Alptekin et. al. [24] developed a natural gas residential heating system able to provide electrical power of 36W. This is one third of the required electrical power of the boiler. An economic analysis revealed that the proposed system is economically applicable. A natural gas boiler was also equipped with TEG for self-powering by Qiu and Hayden [25]. With the maximum electrical power of 161W, their proposed system was capable to provide the electrical power of all electrical components of the boiler. To reach this, a temperature difference between the hot and cold end of the TEG needs to be 214°C. Zheng et. al. [26,27] extended the exhaust gas recovering of boilers by either using the heat of the boiler or providing the heat by solar radiation on the roof. They estimated for the proposed system an annual saving of £213 per domestic boiler and the corresponding cost recovery period of 5.59 years.

Borcuch et. al. [28] examined the influence of the gas heat exchanger cross-sectional geometry with 32 TEG placed, numerically. While comparing five different cross-sections, it turned out that the rectangular cross-section delivers the highest heat flux, but also the highest pressure loss. They proposed a pentagonal cross-section for optimal heat flux and pressure loss. In the analysis of Yan et. al. [29], five cross-sections were also numerically considered. The area available for TEG placement was in all cross sections the same. Although in this study the pumping power of the rectangular cross-section is again the highest, the electrical output power, the net power and the efficiency are at highest, too, compared to the other cross-sections. They determined the maximum net power in the Reynolds number range of 100-500.

Chen et. al. [30] presented a numerical model to predict the performance of rectangular gas heat exchanger equipped with TEG. They predicted that smaller height of the channel increased the velocity and therewith the electric output power (54%) and efficiency (25%). They also predicted, if two TEG are mounted in a tandem, the downstream TEG delivers only 43% of the upstream TEG, whose performance is close to a single TEG setting. This is raised by the reduced gas temperature around the downstream TEG. This reduction of gas temperature can be compensated by a decreasing channel height downstream, as presented by Luo et. al. [31]. The tilt angle of the converging heat exchanger equipped with 16 TEGs can achieve a higher temperature difference and a better TEG output performance. They predicted (numerically) that the tilt angle of 2° is optimal.

Huang and Xu [32] applied a combination of Response Surface Method and genetic algorithm to optimize a heat exchanger equipped with TEG. The TEG is sandwiched between hot and cold gas heat

exchanger with cross flow and counter-flow operation. The study shows the feasibility to maximize the electrical power output of a TEG system.

The present paper reports on the next step of a research project, which addresses biomass combustion in a boiler of 200 kW thermal power as well as cogeneration with thermoelectric generators. In the previous step, a numerical model of the boiler was developed and validated. In the present paper, the focus is on the development and optimization of the boiler heat exchanger equipped with TEG.

## 2 The boiler

The boiler is a wood fuel one with a thermal power of 200 kW. The wood chips are transported by a screw at the furnace bottom. Primary air is injected into the bed of wood chips. The secondary air is injected as jets through a number of nozzles. The combustion products lose heat to boiler walls. To extract the remaining energy and feed this into the water, the gas is conducted through two passes of convective heat exchangers consisting of tubes with twisted tape fittings. The boiler structure is depicted in Figure 1.

## 3 Modelling

The TEG heat exchanger, which is optimized in the present paper, consists out of three parts. The water heat exchanger, the TEG and the gas heat exchanger are sketched in Figure 2.

The three parts are connected through steel plates, which behave like thermal spreader to increase the heat exchanger area of the TEG. The heat exchangers are simple plate heat exchangers because of two reasons. They have low manufacturing costs and are not affected by flue gases with high particle load, compared to fin heat exchanger, which can be blocked by particles. For both heat exchangers, it is important to be designed efficiently in the sense of electrical power requirement. If the energy consumption of the water pump or flue gas blower is too high, the net power of the overall system is not at its maximum.

To maximize the net power a sensitivity analysis was performed which showed that the water pump has a

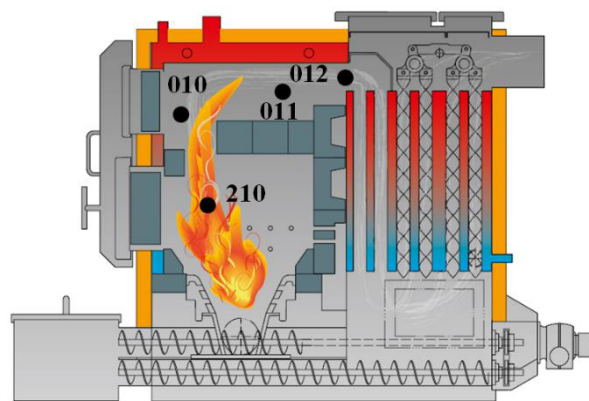


**Fig. 1.** Boiler schematic (indicating some measuring points).

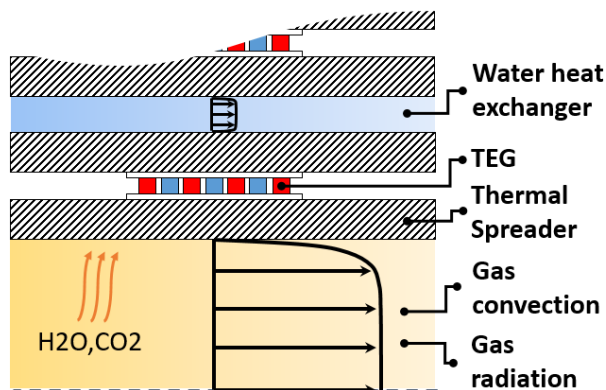


**Fig. 2.** TEG heat exchanger structure.

minor, and the flue gas blower a major influence. This can be explained by the higher volumetric heat capacity of water and the high efficiency of today's heating pumps. The following model focuses on the optimization of the number of TEGs used, their distribution and the design space while changing the gas heat exchanger geometry.

### 3.1 Water heat exchanger

As described before, the water heat exchanger is modelled simplified and therefore implemented as a simple thermal resistance with a heat transfer coefficient of 4500 W/(m<sup>2</sup> K) and a water temperature of 60°C.

### 3.2 TEG model

The heat transport of the TEG is not effected by heat conduction only but additionally by the Peltier effect, Thomson effect and the Joule heating. The TEG should convert heat into electrical power at its maximum power point. A lumped, simplified thermal resistance derived from the data sheet is used to represents the TEG. The values in the data sheet are based on experiments. Thus, all above-mentioned effects are included. In the model, the bismuth telluride based TEG TEP1-24156-24 from Thermanamic Electronics Corp. Ltd. is used [33].

A conversion efficiency plot is provided in the product datasheet and with this and the electrical power output data, a thermal resistance can be derived, as shown in Figure 3. The cold side temperatures are assumed to be within the range of 60°C to 100°C, which

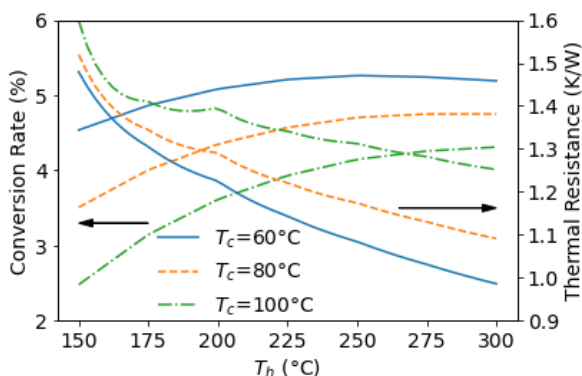


**Fig. 3.** Conversion efficiency and thermal resistance for the used TEG derived from the datasheet [33].

are in the expected range for the described boiler. The thermal resistance decreases when hot side temperature increases or cold side temperature decreases.

### 3.3 Gas heat exchanger

The heat transfer mechanisms acting in the gas heat exchanger are convection and radiation. The flow and forced convective heat transfer in the gas heat exchanger could be modelled by lattice Boltzmann [34] or finite volume method [35] based procedures, as it was previously done for the water heat exchanger. However, with regard to the intended automatic optimization procedure, it was currently found to be more convenient to approximate the forced convective heat transfer with the help of the Gnielinski correlation [36], provided below (the hydraulic diameter of the channel is used in utilizing the correlations).

$$Nu_{m,tu} = \frac{(f/8)RePr}{1 + 12.7\sqrt{f/8}(Pr^{2/3} - 1)} \left[ 1 + \left(\frac{D}{L}\right)^{2/3} \right]$$

$$f = (1.8\log_{10}(Re) - 1.5)^{-2}$$

$$Nu_{m,la} = \left[ 3.66^3 + 0.7^3 + \left( 1.615 \left( RePr \frac{D}{L} \right)^{1/3} - 0.7 \right)^3 \right]^{1/3}$$

$$Nu_{m,tr} = (1 - \gamma)Nu_{m,la,2300} + \gamma Nu_{m,tu,10000}$$

$$\gamma = \frac{Re - 2300}{10000 - 2300}$$

$$Nu_m = \begin{cases} Nu_{m,la}, & \text{if } Re \leq 2300 \\ Nu_{m,tu}, & \text{if } Re > 10000 \\ Nu_{m,tr}, & \text{otherwise} \end{cases}$$

Since the considered flue gas consists partly out of gaseous water and carbon dioxide, radiation effects the heat transfer, especially at the entrance of the heat exchanger where temperatures are high. This effect is described in the model with the emissivity and absorptivity of the “Weighted Sum of Gray Gases Model” (WSGGM) where the coefficients are extracted from Smith et al. [37] and the derived heat transfer coefficient is added to the convective heat transfer coefficient.

### 3.4 Thermal spreader

To increase the area between gas and TEG hot end, steel plates with a larger surface, compared to TEG surface, are used. The thermal spreading effects the thermal resistance of the steel plate. Additionally to the one-dimensional head conductivity of the steel plate a spreading resistance is added [38].

$$r_s = \sqrt{\frac{A_s}{\pi}}, r_p = \sqrt{\frac{A_p}{\pi}}$$

$$\varepsilon = \frac{r_s}{r_p}, \tau = \frac{t}{r_p}, \lambda_c = \pi + \frac{1}{\sqrt{\pi\varepsilon}}$$

$$\Phi_C = \frac{\tanh(\lambda_c \tau) + \frac{k\lambda_c}{hr_p}}{1 + \frac{k\lambda_c}{hr_p} \tanh(\lambda_c \tau)}$$

$$R_p = R_{1D} + R_s = \frac{t}{kA_p} + \frac{(1 - \varepsilon)}{\pi k r_s} \Phi_C$$

## 4 Optimization

The aim of the present investigation is the multi-objective optimization of the TEG gas heat exchanger.

The heat exchanger is modelled in segments, each with a specific setting of design variables. Starting with the segment at the entrance of the heat exchanger a flue gas temperature is assumed. This is used to determine the material properties of the flue gas, the heat extracted from the segment through the TEG, an outlet temperature and an average flue gas temperature of the segment. This is repeated iteratively until a convergence criterion is fulfilled. This is done stepwise downstream until the aimed outlet temperature of 150°C is reached.

A focus of the optimization is the assessment of an exhaust gas recirculation. Exhaust gas is extracted from the outlet and mixed to the inlet of the heat exchanger without influencing the combustion zone. This homogenizes and reduces temperature, increases mass flow rate of the flue gas and therefore increases the heat transfer coefficient. But it also increases the pressure loss and the pumping power of the blower.

### 4.1 Objectives and constraints

Two objectives are considered. Firstly, the design space should be as small as possible. This effects the production and assembling costs, which were not predictable at this point of the project. Secondly, to reduce the costs, the number of TEGs should be as small as possible, too. Additionally, three constraints are needed to be met in designing a practical boiler. The overall electric efficiency should be 3% of thermal power of the boiler. This covers the electrical net power of the system. The minimum height of the heat exchanger should be 1 cm, to avoid the afore-mentioned blocking due to particles. The filling factor needs to be larger than 1, to avoid negative areas. Finally, the TEG hot end surface temperature should not exceed the maximum allowable temperature of 300°C.

### 4.2 Design variables

A sensitivity analysis showed that the following design variables have the highest effect. The height of the channel  $h$  and the ratio between width and height  $w/h$  of the channel describe the inlet geometry, as shown in Figure 4. The height can vary linear with the considered segment and this variation is defined by the design variable  $m_h$ , the slope of the height in flow direction. The filling factor of the TEG  $ff$  is defined as a factor of

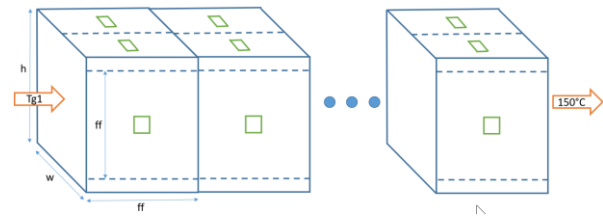


**Fig. 4.** Design variables of the TEG gas heat exchanger model.

the TEG size, which defines the length of the segment in flow direction and additionally it defines the width blocked by one TEG. The design variables, described so far, are defining the number of TEGs per segment. The last design variable is the inlet temperature of the flue gas. As discussed before, this influences the mass flow rate through the heat exchanger, too.

### 4.3 Optimization algorithm

For the present optimization, NOMAD [39] is used. NOMAD is a C++ implementation of the Mesh Adaptive Direct Search algorithm (MADS) [40], designed for difficult black-box optimization problems. These problems occur when the functions defining the objective and constraints are the result of costly computer simulations. It is also capable to optimize bi-objective problems like investigated in the paper.

## 5 Results and discussion

The model described above is solved with the bi-objective optimization algorithm to minimize the design space and the number of TEG. The resulting Pareto front with 50 solutions is shown in Fig. 5. The two points with the minimum design space and with the minimum number of TEG in the Pareto front are marked with a red circle and are discussed. The obtained design variables and the resulting objectives are shown in Table 1. The initial height  $h$  of both solutions is comparable in size. In both cases, due to the negative slope of the height  $m_h$ , the height is at its minimum of 1cm from the second segment on. The larger height at the entrance results from the temperature profile, which is not developed at the entrance of the heat exchanger. As it can be deduced from equations, as the length of the heat exchanger or the number of segments increases the term  $D/L$  and

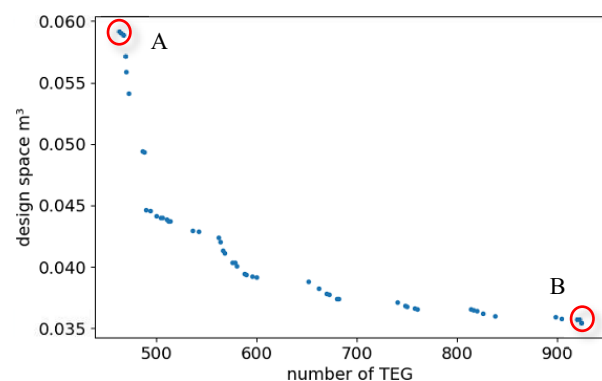


**Fig. 5.** Pareto front of the optimization with the objectives: design space and number of TEG.

thus, the influence of the temperature profile decreases. The w/h ratio of the channel is in both solutions quite high and w is larger than 1m. This underlines the benefit of the rectangular cross-section compared to the square one, as also found by Borcuch et. al. [28] and Yan et. al. [29], since a ratio of one would mean a square cross-section. The inlet gas temperature is in both solutions very close to the maximum gas temperature. This demonstrates the redundancy of the flue gas recirculation in this situation. Although the mass flow rate and the heat transfer coefficient are increased by the recirculation, it seems to be less effective.

The main difference between both solutions is the filling factor. In solution A, the filling factor is slightly above one, but increases rapidly to larger values due to the positive filling factor slope. The increasing filling factor compensates the decreasing flue gas temperature as the upstream TEG extracts heat from the flue gas. In this solution, the hot end of the TEG is nearly constant at 300°C through all TEG segments, as shown in Figure 6a. Things look rather different when we look at the solution B. In solution B the filling factor is initially one and does not change through the segments. Although the filling factor has a negative slope, it does not change as it is already at its minimum. The temperature of the hot end of the TEG is at the entrance at 300°C and is decreasing continuously to non-optimal temperatures (Figure 6b). In Solution A, the TEGs are working with optimal hot side temperatures. This leads to a small number of TEGs but to a long heat exchanger, because the filling factor is increasing continuously. In Solution B, the filling factor is always one. On the one hand, this results in a short heat exchanger, but on the other hand a larger number of TEGs is required to fulfil the aim of having an overall electric efficiency of 3% as the TEGs are not working in an optimal manner.

The other solutions of the Pareto front are in between both extrema of solution A and B. A further step, if known, could be the linkage of both objectives to a single objective, the costs. A larger design space and a larger number of TEGs lead to larger costs.

## 6 Conclusions

A numerical model for a heat exchanger equipped with TEG in a biomass boiler was developed. A bi-objective optimization algorithm optimized the model. The resulting Pareto front shows that the filling factor is the significant variable which defines, whether the space or the amount of TEG is at its minimum. It also shows that a rectangular cross-section at the limit of the constraints, without recirculation is favourable for both objectives. The converging channel is helpful to manage the high heat transfer of a non-developed thermal profile.

## Acknowledgements

The presented results were obtained from the project “Biomasssteg”, which was funded by the funding section “Biomass energy use” of the German Ministry of Economic Affairs and Energy in the framework of the 7. Energy Research Program.

**Table 1.** Two solutions from the Pareto front

| Design Variables    | Solution A | Solution B |
|---------------------|------------|------------|
| h (mm)              | 46.8       | 25.6       |
| w/h                 | 34.7       | 50.0       |
| ff                  | 1.06       | 1          |
| $T_g$ (°C)          | 997        | 987        |
| $m_h$               | -1.8       | -1.31      |
| $m_{ff}$            | 1.63       | -48.6      |
| Objective           |            |            |
| $\eta_{TEG}$        | 462        | 924        |
| V (m <sup>3</sup> ) | 0.0591     | 0.0355     |

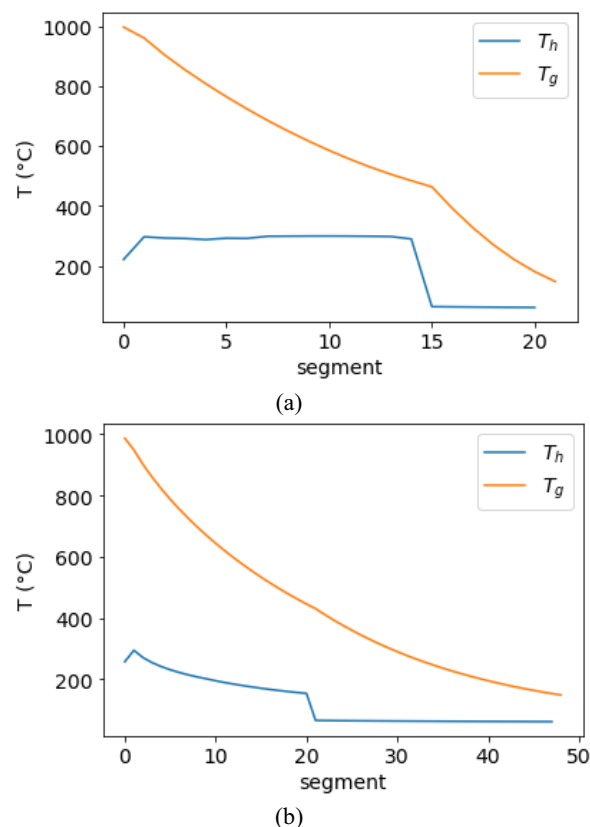


**Fig. 6.** Temperature distribution of flue gas and hot end of TEG in heat exchanger segments, a) solution A, b) sol. B

## References

1. M. Lackner, F. Winter, A. K. Agarwal (Eds), *Handbook of Combustion* (Wiley, Hoboken, 2010)
2. I. Bilousov, M. Bulgakov, V. Savchuk, *Modern Marine Internal Combustion Engines* (Springer, Berlin, 2020)
3. S. Iqbal, A. C. Benim, S. Fischer, F. Joos, D. Kluß, A. Wiedermann, “Experimental and numerical analysis of natural bio and syngas swirl flames in a model gas turbine combustor”, *Journal of Thermal Science* **25(5)** (2016) 460-469
4. A. C. Benim, B. Epple, B. Krohmer, “Modelling of pulverised coal combustion by a Eulerian-Eulerian two-phase flow formulation”, *Progress in Computational Fluid Dynamics – An International Journal* **5(6)** (2005) 345-361
5. B. Epple, W. Fiveland, B. Krohmer, G. Richards, A. C. Benim, “Assessment of two-phase flow models

- for the simulation of pulverized coal combustion”, *International Journal of Energy for a Clean Environment* **6(3)** (2005) 267-287
6. B. Epple, R. Leithner, W. Linzer, H. Walter (Eds), *Simulation von Kraftwerken und Feuerungen* (Springer, Vienna, 2012)
  7. C. Higman, M. van der Burgt, *Gasification*, 2nd ed (Elsevier, Amsterdam, 2008)
  8. R. Ehrlich, *Renewable Energy* (CRC Press, Boca Raton, 2013)
  9. M. S. Tahat, A. C. Benim, “Experimental analysis on thermophysical properties of Al<sub>2</sub>O<sub>3</sub>/CuO hybrid nano fluid with its effects on flat plate solar collector”, *Defect and Diffusion Forum* **374** (2017) 148–156
  10. E. DuBois, A. Mercier (Eds), *Energy Recovery* (Nova Science Publishers, New York, 2009)
  11. S. Bhattacharyya, H. Chattopadhyay, A. C. Benim, “Heat transfer enhancement of laminar flow of ethylene glycol through a square channel fitted with angular cut wavy strip”, *Procedia Engineering* **157** (2016) 19-28
  12. S. Bhattacharyya, A. C. Benim, H. Chattopadhyay, A. Banerjee, “Experimental investigation of heat transfer performance of corrugated tube with spring tape inserts”, *Experimental Heat Transfer* **32(5)** (2019) 411-425
  13. L. Rosendahl (Ed), *Biomass Combustion Science, Technology and Engineering* (Elsevier, Amsterdam, 2013)
  14. M. Kaltschmitt, H. Hartmann, H. Hofbauer, (Eds), *Energie aus Biomasse* (Springer, Berlin, 2016)
  15. A. I. Moreno, R. Font, J. A. Conesa, Combustion of furniture wood waste and solid wood: Kinetic study and evolution of pollutants, *Fuel* **192** (2017)169-177
  16. A. Hepbasli, “A study on estimating the energetic and exergetic prices of various residential energy sources”, *Energy Buildings* **40(3)** (2008) 308–315
  17. E. K. Vakkilainen, *Steam Generation from Biomass* (Elsevier, Amsterdam, 2017)
  18. R. Bauer, M. Göllles, T. Brunner, N. Dourdoumas, I. Obernberger, “Modelling of grate combustion in a medium scale biomass furnace for control purposes”, *Biomass Bioenergy* **34(4)** (2010)417-427
  19. U. Drescher, D. Brüggemann, “Fluid selection for the organic Rankine cycle (ORC) in biomass power plants”, *Appl. Thermal Eng.* **27(1)** (2007) 223-228
  20. H. Liu, Y. Shao, J. Li, “A biomass-fired micro-scale CHP system with organic Rankine cycle (ORC) – Thermodynamic modelling studies”, *Biomass and Bioenergy* **35(9)** (2011) 3985-3994
  21. E. Podesser, “Electricity production in rural villages with a biomass Stirling engine”, *Renewable Energy* **16(1-4)** (1999) 1949-1052
  22. H. Julian Goldsmid, *The Physics of Thermoelectric Energy Conversion* (Morgan & Claypool Publishers, San Rafael, 2017)
  23. K. F. Mustafa, S. Abdullah, M. Z. Abdullah, K. Sopian, “A review of combustion-driven thermoelectric (TE) and thermophotovoltaic (TPV) power systems”, *Renewable and Sustainable Energy Reviews* **71** (2017) 572–584
  24. M. Alptekin, T. Calisir, S. Baskaya, “Design and experimental investigation of a thermoelectric self-powered heating system”, *Energy Conversion and Management* **146** (2017) 244–252
  25. K. Qiu, A. C. Hayden, “Development of thermoelectric self-powered heating equipment”, *J. Electronic Materials* **40(5)** (2010) 606–610
  26. X. F. Zheng, C. X. Liu, R. Boukhanouf, Y. Y. Yan, W. Z. Li, “Experimental study of a domestic thermoelectric cogeneration system”, *Applied Thermal Engineering* **62(1)** (2014) 69–79
  27. X. F. Zheng, Y. Y. Yan, K. Simpson, “A potential candidate for the sustainable and reliable domestic energy generation–Thermoelectric cogeneration system” *Appl. Thermal Eng.* **53(2)** (2013) 305–311
  28. M. Borcuch, S. Gumuła, M. Musiał, K. Wojciechowski, “The analysis of heat exchangers geometry in thermoelectric generators for waste heat utilization”, *E3S Web of Conf.* **10** (2016) 00003
  29. S.-R. Yan, H. Moria, S. Asaadi, H. Sadighi Dizaji, S. Khalilarya, K. Jermsittiparsert, “Performance and profit analysis of thermoelectric power generators mounted on channels with different cross-sectional shapes”, *Appl. Thermal Eng.* **176** (2020) 115455
  30. W.-H. Chen, Y.-X. Lin, Y.-B. Chiou, Y.-L. Lin, X.-D. Wang, “A computational fluid dynamics (CFD) approach of thermoelectric generator (TEG) for power generation”, *Applied Thermal Engineering*, **173** (2020) 115203
  31. D. Luo, R.Wang, W. Yu, Z. Sun, X. Meng, “Modelling and simulation study of a converging thermoelectric generator for engine waste heat recovery”, *Appl. Thermal Eng.* **153** (2019) 837–847
  32. S. Huang, X. Xu, “Parametric optimization of thermoelectric generators for waste heat recovery”, *J. Electronic Materials* **45(10)** (2016) 5213–5222
  33. Thermonamic Electronics (Jiangxi) Corp., Ltd. [Online] <http://www.thermonamic.com/TEP1-24156-2.4-English.pdf>
  34. E. Aslan, I. Taymaz, A. C. Benim, “Investigation of LBM curved boundary treatments for unsteady flows”, *European Journal of Mechanics B/Fluids* **51** (2015) 68-74
  35. A. C. Benim, M. Cagan, A. Nahavandi, E. Pasqualotto, “RANS predictions of turbulent flow past a circular cylinder over the critical regime”, *Proc. 5th IASME/WSEAS International Conference on Fluid Mechanics and Aerodynamics, Athens, Greece, August 25-27, 2007* (2007) 232-237
  36. VDI Heat Atlas (Springer, Berlin, 2010)
  37. T. F. Smith, Z. F. Shen, J. N. Friedman, “Evaluation of coefficients for the weighted sum of gray gases model”, *J. Heat Transfer* **104(4)** (1982) 602–608
  38. Y.-S. Chen, K.-H. Chien, Y.-S. Tseng, Y.-K.- Chan, “Determination of optimized rectangular spreader thickness for lower thermal spreading resistance”, *J. Electronic Packaging* **131(1)** (2009) 011004
  39. C. Audet, S. Le Digabel, C. Tribes and V. Rochon Montplaisir. The NOMAD project. Software available at <https://www.gerad.ca/nomad>
  40. C. Audet and J. E. Dennis, Jr., “Mesh adaptive direct search algorithms for constrained optimization”, *SIAM J. on Optimization* **17(1)** (2006) 188–217